Indian Journal of Pure & Applied Physics
Vol. 62, August 2024, pp. 682-688
DOI: 10.56042/ijpap.v62i8.8860

# Core and Projectile Excitation Effects in $^{12}C(^{31}Cl,^{30}S)X$ Reaction at 44 MeV/nucleon Beam Energy

Sarla Devi & Ravinder Kumar*

Department of Physics, Deenbandhu Chhotu Ram University of Science & Technology, Murthal, Sonipat 131 039 Haryana, India

*Received 16 February 2024; accepted 1 July 2024*

The effects of low-lying core($^{30}S$) and projectile($^{31}Cl$) excited states on the full-width half maxima(FWHM) of longitudinal momentum distribution(LMD) of core fragment and single proton breakup cross-section of $^{12}C(^{31}Cl,^{30}S)X$ breakup reaction at 44 MeV/nucleon beam energy have been analyzed quantitatively for the stripping and diffraction dissociation reaction mechanisms. The calculations are carried out using standard MOMDIS code based on Glauber eikonal approximation. Our analysis shows that the inclusion of core and projectile excitation enhances the LMD width and suppresses the magnitude of the single proton breakup cross-section significantly. Additionally, in comparison with the experimental LMD width, the contribution of *s* and *d*-state in admixed *sd*-state have also been explored. The obtained results are informative for the lucid structural study of the $^{31}Cl$ nucleus.

**Keywords:** Halo breakup; Core excitation; Projectile excitation; Longitudinal momentum Distributions

## Introduction

In 1985, observing exceptionally large matter radii in lithium isotopes opened a new era in nuclear physics research[1] and in the last three decades many neutron/proton-rich nuclei have been artificially produced across the globe for nuclear structure and nucleo synthesis reaction studies[2-5]. These extremely neutron/proton-rich nuclei generally form cluster structures where the valence neutron(s)/proton(s) tunnel out from the range of nuclear forces and form a halo structure that pretends as an extended nucleon distribution. In comparison with neutron halos, proton halos are relatively less pronounced because of Coulomb repulsive interaction between core and valence proton, yet due to the technological advancement in radioactive ion beam (RIB) facilities in last three decades, worldwide, numerous experimental measurements were carried out with neutron deficient nuclei and reported the possibility of existence of proton halo structures such as $^{8}B$, $^{23}Al$, $^{26-28}P$ etc[6-10]. Some of these nuclei have well-understood proton halo structure while many are still under investigation.

Mostly the knockout reactions are employed as an efficient tool for the structural investigations of such exotic nuclei, where the core of the exotic nuclei is frequently treated in their ground state and its significance in nuclear reactions have not been taken seriously, however few theoretical works using Distorted Wave Born Approximation (DWBA), Continuum Discretized Coupled Channels(CDCC), and adiabatic approximation have shown that the core of the exotic nuclei could be in excited state and its inclusion in the calculations creates significant variations in the breakup observable values[11-15] and a better interpretation of experimental data could be achieved with inclusion of core excited/deformed states[16-19]. On the other hand, because of short lifespan and the difficulty in conducting experiments with such excited nuclei, the possibility of the projectile nucleus being in an excited state was neglected and for simplicity, the projectile nuclei were assumed in their ground states. However, few recent experimental observations have shown that some nuclei, such as $^{17}F$, exhibit halo character in their excited states[20-22], and also very recent theoretical investigations have demonstrated the significant roleof inclusion of projectile excited states in the breakup reactions studies[23-25].

In the present study, we have investigated the nuclear breakup of the $^{31}Cl$ nucleus, which is a proton-rich exotic nucleus lying closer to the proton drip line, having very small valence proton separation energy ($S_p$=0.294 MeV)[26] and a long tail in its proton density distribution[27].Besides these properties, a few ambiguities were reported in literature i.e. no

*Corresponding author:
(E-mail: drravinderkumar.phy@dcrustm.org)

enhancement in the interaction cross-section at high energy[28], the composition of $^{31}$Cl with 17 protons and 14 neutrons lies near the region where the possibility of a new proton magic number Z=16 may exist[27,29]. The existence of uncertainty in its proton separation energies *i.e.* $S_p$=294 keV[26]or $S_p$=264.6(±34) keV[30], the possibility of valence proton to occupy*d*-state[26], and more interestingly its role in thermonuclear $^{30}$S(p,γ) $^{31}$Cl reaction in type I X-ray bursts[31] are few issues which attracted the researchers in last few years. As the interpretation of experimental data of breakup reactions provide basic structural information, which are later used to resolving other connective issues. So, more clearly we interpret the data, better information we can reveal about the participating nuclei. Therefore, to explore the nuclear structure of $^{31}$Cl nuclei, a large number of experimental and theoretical studies were carried out in the last two decades[26-28]. Among these investigations, most frequently, the measurement of FWHM of the LMD of core fragment and single proton breakup cross-section were studied and used for revealing its nuclear structure[25,32]. So, keeping in view that the measurement of FWHM of LMD of core fragment and single proton knockout cross-section are one of cleaner probes, frequently used for revealing the structural information of exotic nuclei and the absolute magnitude of these observable are very much sensitive to the core and projectile excitation energies as shown in[Ref.24,25].

Therefore, it is quite interesting to examine quantitatively the sensitivity of these observable with core and projectile excitation energies in $^{12}$C($^{31}$Cl,$^{30}$S)X reaction for revealing clear structural information of the $^{31}$Cl nucleus. With this motivation, we calculated and analyzed these observables with the ground and the recently reported core excited states *i.e.* $2_1^+(E_x^c$=2.21 MeV), $2_2^+(E_x^c$=3.40 MeV), $1_1^+(E_x^c$=3.67 MeV)[33] and also the projectile excited state $J^\pi = 1/2^+$ ($E_x^p$=0.737 MeV)[34]. The brief details of the theoretical formalism are discussed in Sec. 2, obtained results and their interpretations are shown in Sec. 3, and conclusions are presented in Sec. 4.

## 2 Theoretical Formalism

We proceed with the assumption that the $^{31}$Cl nucleus consists of a core plus valence proton system and in the case of the $^{12}$C target, the breakup is caused due to the dominating stripping and diffraction dissociation mechanisms[35,36]. The LMD of the core fragment and single proton breakup cross-section in stripping and diffraction dissociation mechanisms are calculated using MOMDIS code[37] based on the Glauber eikonal Model[37,38]. This code is suitable for single nucleon knockout reaction studies at intermediate to high beam energies. Following the theoretical formalism discussed in[Ref.37,40], the momentum distribution in stripping (or inelastic) and diffraction mechanisms are calculated using Eqs 1 & 2, and respective LMD is obtained by integrating the Eqs 1 & 2 over the transverse components of k. The coordinate system used in the calculation is shown in[Ref.41,42].

$$\frac{d\sigma^{str}}{d^3k} = \frac{1}{(2\pi)^3}\frac{1}{2L_0+1}\sum_{M_0}\int d^2\,b_n\,[1 - |S_n(b_n)|^2]\left|\int d^3r\, e^{-ik.r} S_c(b_c)\phi_{0,M_0}(r)\right|^2 \quad \ldots (1)$$

$$\frac{d\sigma^{diff}}{d^3k} = \frac{1}{(2\pi)^3}\frac{1}{2L_0+1}\sum_{M_0}\int d^2\,b_c\left|\int d^3r e^{-ik.r}\, S_c(b_c)S_n(b_n)\phi_{0,M_0}(r)\right|^2 \quad \ldots (2)$$

The single proton breakup cross sections are obtained by integrating Eqs 1 & 2 over all the components of the momentum (***k***), shown in Eq. 3 (for stripping) and Eq. 4 (for diffraction)[37-40]

$$\sigma^{str} = \frac{1}{2L_0+1}\sum_{M_0}\int d^2\,b_n[1 - |S_n(b_n)|^2]\int d^3r\,\phi_{0,M_0}(r)^*|S_c(b_c)|^2\phi_{0,M_0}(r) \quad \ldots(3)$$

$$\sigma^{diff} = \frac{1}{2L_0+1}\sum_{M_0}\int d^2b_c\left[\int d^3\,r\phi_{0,M_0}(r)^*|S_c(b_c)S_n(b_n)|^2\phi_{0,M_0}(r) - \sum_{M_0'}\left|\int d^3r\,\phi_{0,M_0'}(r)^* S_c(b_c)S_n(b_n)\phi_{0,M_0}(r)\right|^2\right] \quad \ldots (4)$$

Here, $S_c(b_c)$ and $S_n(b_n)$ are the core target and proton target S-matrices (Profile functions), calculated using the HF nuclear density forms of core and target nuclei[43]. The symbols $b_c$ and $b_n$ are the core-target and valence nucleon–target impact parameters. The single particle bound state wave function of the projectile (core plus proton) *i.e.* $\phi(r)$), appearing in Eqs 1-4, is specified as $\phi(r) = R_l(r)Y_{lm}(\hat{r})$, where $R_l(r)$ and $Y_{lm}(\hat{r})$ are the radial wave function and spherical harmonics respectively. The radial wave functions for each considered projectile configuration are calculated by

numerically solving the Schrodinger equation using Wood-Saxon (WS) nuclear potential. For the assumed projectile configurations, the depth of nuclear potential is fitted to reproduce the effective separation energy ($S_p^{eff}$=$S_p$+$E_x^c$-$E_x^p$) of valance proton, where $S_p$, $E_x^c$ and $E_x^p$ are the single proton separation energy in ground state, core and projectile excitation energies respectively. The WS potential radii parameter ($r_0$), diffuseness ($a_0$), and Spin-Orbit potential ($V_{ls}$) are kept fixed at 1.27 fm, 0.67 fm, and 17 MeV, respectively, for all the considered projectile configurations as used in [Ref.[26]]. $L_0$ and $M_0$ are the orbital angular momentum and its projections of valence proton in projectile. Further details of theoretical formalism are discussed in[Ref.37-40]. Keeping in view that projectile wave function is quite sensitive to the WS potential parameters, so before proceeding to the final calculations, we checked the sensitivity of LMD width and proton breakup cross-section on WS potential parameters for one of projectile's configuration case, and found that as the range parameter ($r_0$) varies from 1.17 fm to 1.37 fm and diffuseness ($a_0$) from 0.57 fm to 0.77 fm, the breakup observables varies approximately by 5%, as reported in[Ref.24,25].

## 3 Results and Discussion

Using the above theoretical formalism, we calculated the momentum distribution of core ($^{30}$S) and single proton breakup cross-section for $^{31}$Cl nucleus projected on $^{12}$C target at 44 MeV/nucleon beam energy. We have analyzed the effect of the inclusion of newly reported core and projectile excited state[33,34] in the theoretical calculations of FWHM of LMD and single proton breakup cross-section.

Since this nucleus is reported to have a core plus valence proton halo structure with large ambiguity of orbital occupancy of valence proton to be either in pure *s*-state or pure *d*-state or admixed *sd*-state, so we performed calculations for several possible core plus valence proton projectile configurations as per the nuclear shell model predictions, in which valence proton may lay either in $2s_{1/2}$ or $1d_{3/2}$ or $1d_{5/2}$ state with the possibility of core and projectile to be in the ground state or excited state[33,34]. We used the reported core excited states $2_1^+$($E_x^c$=2.21 MeV), $2_2^+$($E_x^c$=3.40MeV) and $1_1^+$($E_x^c$=3.67 MeV)[33] as well as projectile ($^{31}$Cl) excited state $J^\pi$=1/2$^+$ ($E_x^p$=0.737 MeV)[33,34] for the calculations of LMD and breakup cross section. The calculated results for different core plus valence proton configurations for ground $J^\pi$=3/2$^+$($E_x^p$=0.0MeV) and excited state $J^\pi$=1/2$^+$ ($E_x^p$=0.737MeV) of the projectile are shown in Table 1 & 2, respectively. In these tables, first column shows the assumed core⊗proton projectile configurations, second column the depth of Woods-Saxon potential ($V_0$), third column rms radii, fourth column the core excitation energy ($E_x^c$), and fifth column shows the effective binding energy of valence proton ($S_p^{eff}$) the calculated single proton breakup cross-section and FWHM of LMD of core fragment after the breakup of $^{31}$Cl in stripping plus diffraction breakup mechanism are shown in sixth and seventh columns, respectively. For the projectile's ground state *i.e.* $J^\pi$=3/2$^+$($E_x^p$=0.0 MeV), we assumed that thestate could be produced either by core ground state i.e. 0$^+$ (0.0 MeV) or any excited state *i.e.* $2_1^+$(2.21 MeV), $2_2^+$(3.40 MeV), $1_1^+$ (3.67 MeV), coupled with $2s_{1/2}$, or $1d_{3/2}$ or $1d_{5/2}$ state of valence proton as per the

Table 1 — Calculated single proton breakup cross-section and Full Width Half Maxima(FWHM) width of LMD in the nuclear breakup (stripping and diffraction dissociation mechanism) of $^{31}$Cl, for various bound state projectile configurations, in projectile's ground state, $J^\pi$= 3/2$^+$ ($E_x^p$=0.0 MeV).

| [Core⊗Proton] (Configuration) | $V_0$ (MeV) | rms radii (fm) | $E_x^c$ (MeV) | $S_p^{eff}$ (MeV) | Cross-section (mb) | FWHM of LMD (MeV/c) |
|---|---|---|---|---|---|---|
| $2_1^+\otimes 2s_{1/2}$ | 47.37 | 4.09 | 2.21 | 2.50 | 38.88 | 89.75 |
| $2_2^+\otimes 2s_{1/2}$ | 49.55 | 3.93 | 3.40 | 3.69 | 33.71 | 96.79 |
| $1_1^+\otimes 2s_{1/2}$ | 50.05 | 3.91 | 3.67 | 3.97 | 32.75 | 98.23 |
| $0^+\otimes 1d_{3/2}$ | 48.14 | 3.86 | 0.0 | 0.29 | 28.26 | 202.93 |
| $2_1^+\otimes 1d_{3/2}$ | 51.72 | 3.65 | 2.21 | 2.50 | 22.35 | 230.37 |
| $2_2^+\otimes 1d_{3/2}$ | 53.57 | 3.57 | 3.40 | 3.69 | 20.43 | 240.83 |
| $1_1^+\otimes 1d_{3/2}$ | 53.99 | 3.56 | 3.67 | 3.97 | 20.05 | 243.02 |
| $2_1^+\otimes 1d_{5/2}$ | 41.98 | 3.88 | 2.21 | 2.50 | 27.32 | 223.93 |
| $2_2^+\otimes 1d_{5/2}$ | 44.02 | 3.79 | 3.40 | 3.69 | 24.85 | 233.94 |
| $1_1^+\otimes 1d_{5/2}$ | 44.48 | 3.77 | 3.67 | 3.97 | 24.36 | 236.02 |

Table 2 — Same as Table 1, but for projectile's excited state, $J^{\pi}= 1/2^{+}$ ($E_x^p$=0.737 MeV).

| [Core⊗Proton] (Configuration) | $V_0$ (MeV) | rms radii (fm) | $E_x^c$ (MeV) | $S_p^{eff}$ (MeV) | Cross-section (mb) | FWHM of LMD (MeV/c) |
|---|---|---|---|---|---|---|
| $1_1^+ \otimes 2s_{1/2}$ | 48.72 | 3.99 | 3.67 | 3.23 | 35.49 | 94.21 |
| $2_1^+ \otimes 1d_{3/2}$ | 50.54 | 3.71 | 2.21 | 1.77 | 23.87 | 222.76 |
| $2_2^+ \otimes 1d_{3/2}$ | 52.43 | 3.62 | 3.40 | 2.96 | 21.55 | 234.59 |
| $1_1^+ \otimes 1d_{3/2}$ | 52.86 | 3.60 | 3.67 | 3.23 | 21.11 | 237.01 |
| $2_1^+ \otimes 1d_{5/2}$ | 40.69 | 3.95 | 2.21 | 1.77 | 29.26 | 216.64 |
| $2_2^+ \otimes 1d_{5/2}$ | 42.77 | 3.85 | 3.40 | 2.96 | 26.29 | 227.96 |

shell model predictions. So, the possible core plus proton bound state configurations are considered and listed in Table 1, respective configuration wise calculated values of FWHM of LMD (seventh columns) and single proton breakup cross section values (sixth column) are also listed in Table 1. Here, for the sake of simplicity, we took the spectroscopy factor as unity for each configuration. It is clear from the Table 1, that the calculated FWHM of LMD corresponding to $2s_{1/2}$ wave configuration is too narrow, while of $1d_{3/2}$ and $1d_{5/2}$ states are much wider momentum distribution than that of the experimental value 158±40 MeV/c[26]. However, as far as breakup cross-section is concern, *s*-wave configurations show the highest breakup cross section than that of *d*-states, which is quite expected for *s*-state because of having no centrifugal potential the valence nucleon forms a more extended system and hence more breakup cross-section and narrow momentum distribution is expected. So, the calculated results show that none of the pure *s* or *d*-states with possible ground or excited core states could reproduce the experimental width *i.e.* 158±40 MeV/c[26].

However, the role of the core excitation is found effective in both the observable magnitudes *i.e.* with increase in core excitation energy the breakup cross section decreases and LMD width increases significantly. A similar trend of results is observed for the projectile excited state ($J^{\pi}=1/2^{+}$), as can be seen in Table 2. For the sake of clarity, the variation in breakup cross-section and FWHM width of LMD distribution with core excitation energies are shown in Fig. 1(a-d) for the ground state ($3/2^{+}$, $E_x^p$ =0.0 MeV) of the projectile and in Fig. 1(e-f) for the excited state ($1/2^{+}$, $E_x^p$ =0.737 MeV). It is noticed that for both the projectile states that the variation in magnitude of observables with rise in core excitation energy is almost linear. Quantitatively, the single proton breakup cross-section reduces approximately 11% and 7-8% with per MeV core excitation energy while the FWHM of LMD width increases approximately 6% and 3-5% with per MeV core excitation energy, for pure *s* or *d*-states, respectively. Also, the effect of inclusion of projectile excitation energy can be noticed in Table 1 & 2 that due to projectile excitation the single proton breakup cross-section enhances approximately by 5-8% and the LMD width reduces approximately by 2-4% for both *s* and *d*-states. It is important to mention that the measurement of FWHM of LMD width has been a very reliable tool for nuclear structural studies[32]. So, it would be interesting to investigate further the LMD for this reaction to reveal the orbital occupancy of valence proton in $^{31}$Cl. The calculated FWHM of LMD shown in Table 1 & 2, clearly shown that pure *s* or pure *d*-states are unable to reproduce the experimental FWHM width of the LMD spectrum[26], even the inclusion of core excited state can reproduce the experimental LMD width *i.e.* 158±40 MeV/c. So, this observation strongly reflects the possibility of having an admixed *sd*-state in $^{31}$Cl nucleus, as pointed in[Ref.26]. But interestingly, so far, the contribution of *s* and *d*-state in *sd* state has not been studied quantitatively for $^{31}$Cl. Therefore, we have examined the contribution of pure *s* and *d*-state in admixed *sd*-state (in terms of percent), which better reproduces the experimental LMD width. Fig. 2 shows the admixing of pure $2s_{1/2}$ configurations with $1d_{3/2}$ or $1d_{5/2}$ configurations (shown on the x-axis) for the projectile ground state $J^{\pi}=3/2^{+}$($E_x^p$ =0.0 MeV). Here, *s* and *d*-states are considered with various core excited states *i.e.* $2_1^+$, $2_2^+$and $1_1^+$. The shaded region in these figures represents the experimental FWHM width of LMD with error bar. Fig. 2(a) shows the mixing of $2s_{1/2}$ with $1d_{3/2}$, whereas Fig. 2(b), shows the mixing of $2s_{1/2}$ and $1d_{5/2}$ configurations, respectively, and the obtained percent contributions of pure *s* and *d*-states are shown in respective legends. It is clearly seen from Fig. 2(a) that the contribution of

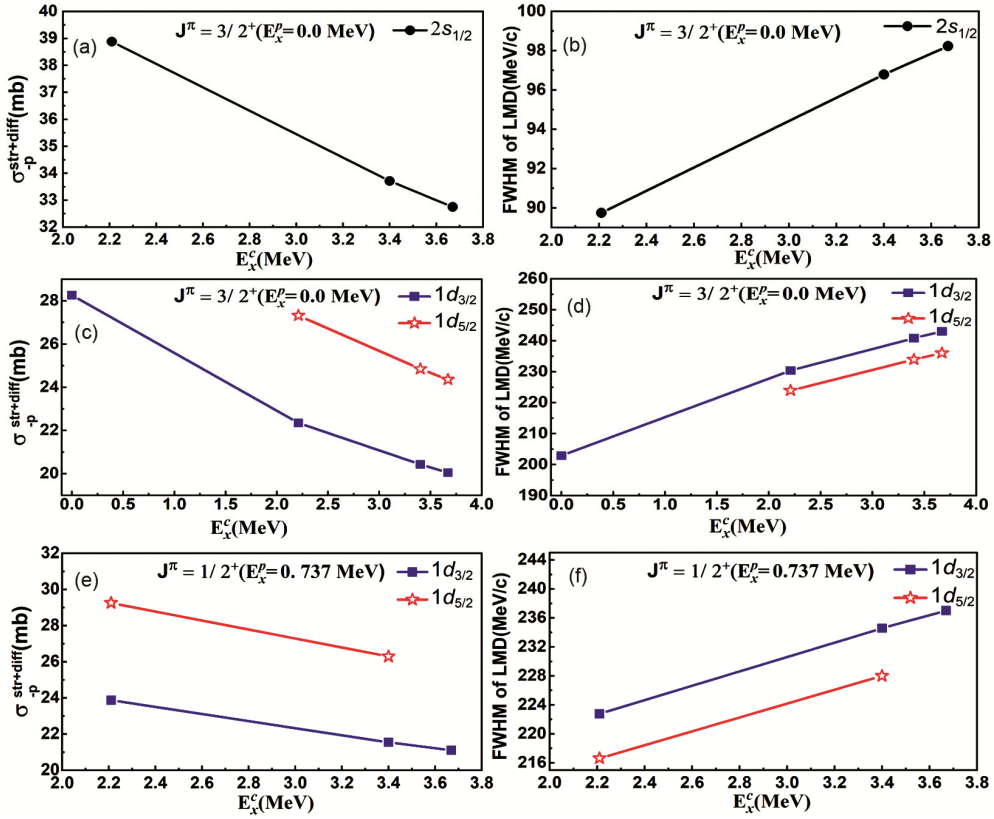


Fig. 1 — (Color online) The variation of single proton cross-section and FWHM of LMD distribution (in stripping plus diffraction dissociation mechanism) with core excitation energy for pure *s* and *d*-states

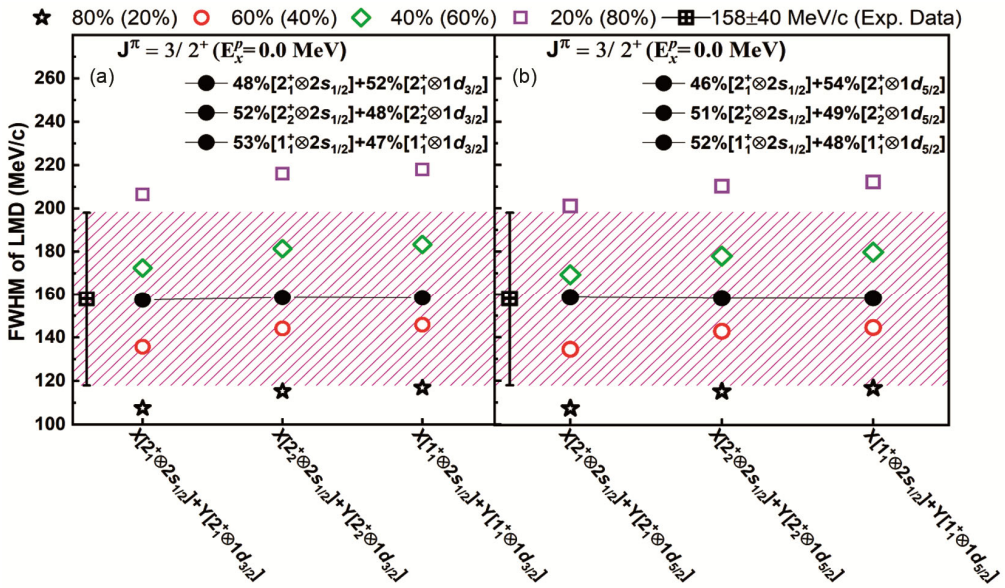


Fig. 2 — (Color online) Admixing of *s* and *d* states for ground state of $^{31}$Cl, $J^\pi = 3/2^+$ ($E_x^p$=0.0MeV)with core excited states (a) shows mixing of $2s_{1/2}$ with $1d_{3/2}$ states while (b) shows mixing of $2s_{1/2}$ with $1d_{5/2}$ states, different symbol shows the percentage contribution of $2s_{1/2}$ and $1d_{3/2}$ or $1d_{5/2}$ states in *s*%(*d*%) syntax on top, the dummy symbols X and Y on the x-axis with configuration shows the percent contribution of each pures or *d*-configuration. The obtained good fit contributions are shown in legend (with black filled dots in figures). Experimental LMD width is taken from[Ref.26]

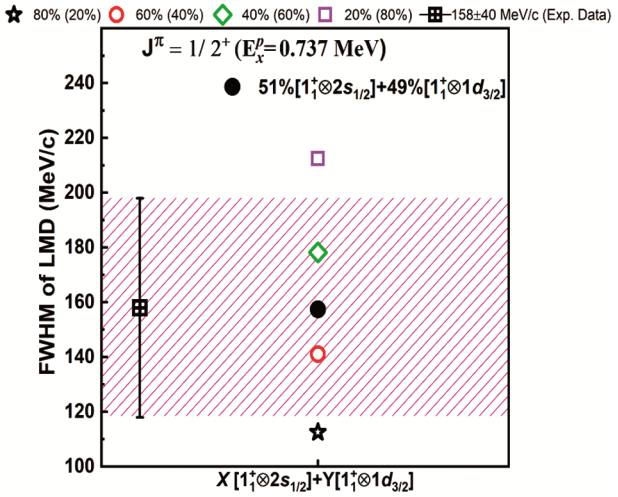


Fig. 3 — (Color online) Same as Fig. 2, but for excited state, $J^{\pi}= 1/2^{+}$ ($E_x^p$=0.737 MeV) of $^{31}Cl$

$2s_{1/2}$ state lying between 48% to 53% and of $1d_{3/2}$ it is between 52% to 47%, which provide a good fit to the experimental LMD width (mean value) *i.e.* 158 MeV/c. Similarly, the Fig.2(b) show that, the contribution of $2s_{1/2}$ lying between 46% to 52%, and of $1d_{5/2}$ is 54% to 48%. The effect of core excitation on the contributions of *s* and *d*-states in admixed state is noticed very small. Similarly, the sharing of *s* and *d*-states is also examined for the projectile excited state $J^{\pi}=1/2^{+}$($E_x^p$=0.737 MeV) as shown in Fig. 3, here the contribution of $2s_{1/2}$ and $1d_{3/2}$ is found around 51% and 49%, respectively, which provide a good fit to the mean value of experimental FWHM of LMD. So, this analysis of mixing of pure *s* and *d*-states configurations, strongly confirm the existence of the *sd*-shell in $^{31}Cl$, and approximate equal contribution of pure *s* and *d*-states gives good fit to the experimental LMD width. Also, from Figs. 2 & 3 it can be noticed that the percent contribution of *s* or *d*-state in admixed *sd*-state, is feebly influenced by the core and projectile excitation. Here, we have not examined the existence of proton in $1d_{3/2}$ or $1d_{5/2}$ state, which would be analyze in our forthcoming work.

## 4 Conclusion

The effect of core and projectile excited states on the LMD width of core fragment and single proton breakup cross-section have been analyzed quantitatively for single proton knockout reaction $^{12}C(^{31}Cl,^{30}S)X$ at 44 MeV/nucleon incident energy, in stripping and diffraction breakup mechanisms using the MOMDIS code. We have used the recently reported core and projectile excited states for the calculations of breakup observables. The obtained results show that with rise in core excitation energy, single proton knockout cross-section decrease by ~7-11% and width of LMD spectrum increase by ~3-6% with per MeV core excitation energy. The inclusion of projectile low-lying excitation energy indeed enhances the breakup cross section approximately by 5-8%, while the LMD width reduce approximately by 2-4% for both *s* or *d*-states. Additionally, it is found that none of pure *s* or *d*-states with the ground or excited state of the core can reproduce the experimental LMD width and single proton breakup cross-section, which is substantial evidence of the presence of *sd*-shell in $^{31}Cl$. Our analysis of the mixing of pure *s* or *d* state confirms that there exists an almost equal contribution of *s* or *d*-state in *sd*-shell that provide a good fit to the experimental FWHM of LMD distribution, dominancy of *d*-state has not been observed in our analysis as reported in[Ref.26]. Finally, we conclude that our work presented a quantitative study to reflect the significant role of core and projectile low-lying excited state in the theoretical calculations of breakup observable of $^{31}Cl$ nucleus. Further, we found strong evidence of existence of *sd*-shell with almost equal contribution of *s* or *d*-state. With these findings, we believe that our quantitative analysis would not only be helpful for the better interpretation of breakup data of $^{31}Cl$ nucleus, but also help full for other breakup reaction involving exotic nuclei.

## Competing Interests

The authors declare no competing financial interest.

## Acknowledgment

Sarla Devi, one of the authors, is grateful to CSIR: Council of Scientific and Industrial Research, New Delhi for the financial support as a Senior Research Fellow (SRF) via reference number 09/1063(0029)/2019-EMR-I.

## References

1 Tanihata I, Hamagaki H, Hashimoto O, Nagamiya S, Shida Y, Yoshikawa N, Yamakawa O, Sugimoto K, Kobayashi T, Greiner DE & Takahashi N, *Phys Lett B*, 160 (1985) 380.

2 Kamigaito O, *IPAC2013: Proc of the 4th Inter Part Acc Conf,* (2013)12.

3 Li B, Tang N, Zhang Y H & Zhang F S, *Nucl Sci Tech*, 33 (2022) 55.

4 Langanke K, *EPJ Web of Conf*, EDP Sciences, 284 (2023) 03001.
5 Yamaguchi H, Hayakawa S, MaNR, Shimizu H, Okawa K, Zhang Q, Yang L, Kahl D, La Cognata M, Lamia L & Abe K, *EPJ Web of Conf*, EDP Sciences, 275 (2023) 01015.
6 Negoita F, Borcea C, Carstoiu F, Lewitowicz M, Saint-Laurent M G, Anne R, Bazin D, Corre J M, Roussel-Chomaz P, Borrel V, Guillemaud-Mueller D, *Phys Rev C*, 54 (1996) 1787.
7 Navin A, Bazin D, Brown B A, Davids B, Gervais G, Glasmacher T, Govaert K, Hansen P G, Hellström M, Ibbotson R W & Maddalena V, *Phys Rev Lett*, 81 (1998) 5089.
8 De-Qing F, Chun-Wang M, Yu-Gang M, Fang D Q, Ma C W, Ma Y G, Cai X Z, Chen J G, Chen J H, Guo W, Tian W D, Wang K, Wei Y B & Yan T Z, *Chin Phys Lett*, 22 (2005) 572.
9 Zu-Hua L, Ming R, Yao-Lin Z, Huan-Qiao Z, Feng Y, Zhong-Yu M, Cheng-Jian L, Bao-Qiu C, Yue-Wei W, Wen-Long Z & Zhong-Yan G, *Chin Phys Lett*, 21 (2004) 1711.
10 Ni D D & Ren Z Z, *Chin Phys C*, 41 (2017) 114104.
11 Tostevin J A, *J Phys G: Nucl Part Phys*, 25 (1999) 735.
12 MoroA M & Crespo R, *Phys Rev C*, 85 (2012) 054613.
13 Shyam R & Danielewicz P, *Phys Rev C*, 63 (2001) 054608.
14 MoroA M & Lay J A, *Phys Rev Lett*, 109 (2012) 232502.
15 Gómez-Ramos M, Moro A M, Gómez-Camacho J & Thompson I J, *Phys Rev C*, 92 (2015) 014613.
16 Nunes F M, Thompson I J & Johnson R C, *Nucl Phys A*, 596 (1996) 171.
17 Summers N C, Nunes F M & Thompson I J, *Phys Rev C*, 74 (2006) 014606.
18 Batham P, Thompson I J & Tostevin J A, *Phys Rev C*, 71 (2005) 064608.
19 Chatterjee R & Shyam R, *Prog Part Nucl Phys*, 103 (2018) 67.
20 Morlock R, Kunz R, Mayer A, Jaeger M, Müller A, Hammer J W, Mohr P, Oberhummer H, Staudt G & Kölle V, *Phys Rev Lett*, 79 (1997) 3837.
21 Belyaeva T L, Goncharov S A, Demyanova A S, Ogloblin A A, Danilov A N, Maslov V A, Sobolev Y G, Trzaska W, Khlebnikov S V, Tyurin G P & Burtebaev N, *Phys Rev C*, 98 (2018) 034602.
22 Demyanova A S, Danilov A N, Ogloblin A A, Goncharov S A, Belyaeva T Y L, Trzaska W H & Starastsin V I, *JETP Lett*, 112 (2020) 463.
23 Ogloblin A A, Danilov A N, Belyaeva T L, Demyanova A S, Goncharov S A & Trzaska W, *Phys Rev C*, 84 (2011) 054601.
24 Devi S & Kumar R, *Phys Par Nucl Lett*, 20 (2023) 17.
25 Shubhchintak, *Phys Rev C*, 96 (2017) 024615.
26 Fu Y, Fang D Q, Ma Y G, Cai X Z, Tian W D, Wang H W, Guo W, Liu G H, Ma C W, Fan R R & Fu F, *Phys Rev C*, 84 (2011) 037603.
27 Xiang-Zhou C, Wen-Qing S, Zhong-Zhou R, Wei-Zhou J, De-Qing F, Hu-Yong Z, Chen Z, Yi-Bin W, Wei G, Yu-Gang M & Zhi-Yuan Z, *Chin Phys Lett*, 19 (2002) 1068.
28 Ozawa A, Baumann T, Chulkov L, Cortina D, Datta U, Fernandez J, Geissel H, Hammache F, Itahashi K, Ivanov M & Janik R, *Nucl Phys A*, 709 (2002) 60.
29 Ozawa A, Kobayashi T, Suzuki T, Yoshida K & Tanihata I, *Phys Rev Lett*, 84 (2000) 5493.
30 Kankainen A, Canete L, Eronen T, Hakala J, Jokinen A, Koponen J, Moore I D, Nesterenko D, Reinikainen J, Rinta-Antila S & Voss A, *Phys Rev C*, 93 (2016) 041304.
31 Togano Y, Motobayashi T, Aoi N, Baba H, Bishop S, Cai X, Doornenbal P, Fang D, Furukawa T, Ieki K & Iwasa N, *J Phys: Conf Ser*, 312 (2011) 042025.
32 Sauvan E, Carstoiu F, Orr N A, Winfield J S, Freer M, Angélique J C, Catford W N, Clarke N M, Curtis N, Grévy S & Le Brun C, *Phys Rev C*, 69 (2004) 044603.
33 National Nuclear Data Center(NNDC), (2009)URL: *www.nndc.bnl.gov*
34 Chen J & Singh B, *Nucl Data Sheets*, 184 (2022) 29.
35 Serber R, *Phys Rev*, 72 (1947) 1008.
36 Glauber R J, *Phys Rev*, 99 (1955) 1515.
37 Bertulani C A & Gade A, *Comp Phys Comm*, 175 (2004) 372.
38 Shukla P, *Phys Rev C*, 67 (2003) 054607.
39 Abu-Ibrahim B, Ogawa Y, Suzuki Y & Tanihata I, *Comp Phys Commun*, 151 (2003) 369.
40 Hencken K, Bertsch G & Esbensen H, *Phys Rev C*, 54 (1996) 3043.
41 Kumar R & Bonaccorso A, *Phys Rev C*, 84 (2011) 014613.
42 Aumann T, Barbieri C, Bazin D, Bertulani C A, Bonaccorso A, Dickhoff W H, Gade A, Gómez-Ramos M, Kay B P, Moro A M & Nakamura T, *Prog Part Nucl Phys*, 118 (2021) 103847.
43 Nuclear Data Services, accessed (2009)RIPL-3: Reference Input Parameter Library (iaea.org).